Orientational Dependence of Charge Transport in Disordered Silicon Nanowires

ARTICLE *in* NANO LETTERS · JANUARY 2009

Impact Factor: 13.59 · DOI: 10.1021/nl801128f · Source: PubMed

Orientational Dependent Surface Roughness Effects in Silicon-based Semiconducting Nanowires

Martin P. Persson,[1] Aurélien Lherbier,[1,2] Yann-Michel Niquet,[1] François Triozon,[3] and Stephan Roche[4]

[1] *CEA/DSM/DRFMC/SP2M/L_Sim, 17 rue des Martyrs, 38054 Grenoble Cedex 9, France*
[2] *Laboratoire des Technologies de la Microélectronique (LTM), UMR 5129 CNRS, CEA 17 Rue des Martyrs 38054 Grenoble France*
[3] *CEA LETI-MINATEC, 17 rue des Martyrs, 38054 Grenoble, Cedex 9 France*
[4] *CEA/DSM/DRFMC/SPSMS/GT, 17 rue des Martyrs, 38054 Grenoble Cedex 9, France*

(Dated: February 11, 2008)

We report on a theoretical study of surface roughness effects on charge conduction in silicon nanowires with three difference crystalline orientations, [100], [110] and [111]. Using an atomistic tight-binding model, transport properties are investigated with both the Kubo-Greenwood and Landauer-Büttiker approaches. Key transport features such as mean-free path, charge mobility and conductance scaling are derived. The large difference in electronic structure between the different nanowire crystal orientations result in strong orientational dependence of the fundamental roughness-induced transport length scales.

"Bottom-up" fabricated semiconducting nanowires have become the subject of intense study and are considered as potential building blocks for nanoscale electronics due to their promising electronic and optical properties.[1] Recent progress in nanowire growth techniques have produced high quality silicon nanowires allowing for new and innovative device designs. Demonstrations of p-n junction diodes,[2] logic gates,[3] field effect transistors,[4, 9] and nanosensors [5] have already been reported. Silicon nanowires (SiNWs) are of particular interest due to their prominent role in the miniaturization of MOSFET devices.[6] Compared to classical planar technology, SiNWs are able to better accommodate "all-around" gates, which improves field effect efficiency and device performance.[7–9] Also, in contrast to many other nanowire materials, structurally stable and electrically active SiNWs can be manufactured with small diameters $d < 5$ nm.[10]

However, as the lateral size of the nanowires becomes smaller the impact of structural imperfections such as surface disorder and defects becomes increasingly important due to the high surface to volume ratio. In the case of lithographic SiNW-FETs surface roughness disorder (SRD) is known to be a limiting factor.[11, 12] Moreover, due to the indirect band gap of silicon, SiNWs can be expected to exhibit fundamentally different electronic properties depending on the nanowire crystal orientation. For engineering of performant SiNW-based transistors it is thus imperative to find out how sensitive the transport properties are to SRD and which nanowire orientation is best suited for engineering highly performant transistors.

Recent studies of SiNWs have shown that the band structure and related properties are strongly dependent on the crystal orientation of the nanowire.[13] The role of disorder has been investigated either with *ab initio* approaches [14, 15], or with more phenomenological models.[16, 17] The latter do not include the full band structure, essential to achieve a quantitative understanding of charge transport in realistic disordered SiNWs. In contrast, while the *ab initio* studies describe the full band structure, they remain computationally too demanding and can generally not give access to the fundamental transport length scales.

In this Letter, we report on a comparative study of transport properties of SiNWs oriented along the [100], [110] and [111] crystal directions taking into account surface roughness effects. The SiNWs are modelled using an accurate atomistic sp^3 third nearest neighbor tight-binding Hamiltonian with hydrogen surface passivation, previously validated by *ab initio* calculations.[13] The tight-binding method has the two fold advantage of accurately describing the bandstructure and of being computationally less demanding than *ab initio* methods. Following a prior work,[18] two complementary approaches are used to explore the conduction regimes in disordered SiNWs; namely an order N Kubo-Greenwood approach which gives a straightforward access to the intrinsic elastic mean free path and charge mobility [19], together with a Landauer-Büttiker approach to compute the quantum conductance, particularly useful in the quasi-ballistic regime, where contact effects start to prevail over intrinsic phenomena.

The SiNW SRD profile is defined as a random fluctuation of the nanowire radius around its average value R_0, characterized by a Lorentzian auto-correlation function.[12, 18, 20] Any atom outside the surface profile is removed and the dangling bonds are saturated with hydrogen atoms. In cylindrical coordinates the profile reads

$$\delta R(z,\theta) = \sum_{(n,k)\neq(0,0)} a_{nk}\, e^{in\theta}\, e^{i\frac{2\pi}{L}kz}, \qquad \text{(1a)}$$

where

$$a_{nk} = e^{i\varphi_{nk}} \left\{ 1 + \left[\left(\frac{2\pi k}{L}\right)^2 + \left(\frac{n}{R_0}\right)^2 \right] L_r^2 \right\}^{-3/4}. \qquad \text{(1b)}$$

$\varphi_{nk} \in [0, 2\pi[$ is a random number and L_r is the correlation length of the SRD and L is the length of the nanowire. In the following, we set $R_0 = 1$ nm while the a_{nk} are renormalized such that $\left\langle \delta R^2(z,\theta) \right\rangle^{1/2} = 1$ Å. The effects of the SRD on the transport length scales have been analyzed for SiNWs with $L_r = 2.17$ nm. An example of the SRD is shown in Fig. 3(a).

The band structures and densities of states (DoS) for ideal SiNWs, with diameters of 2 nm, are shown in Fig. 1. The basic characteristics for the band structure of SiNWs oriented along [100], [110] and [111] directions are collected in table I. Since bulk silicon is an indirect band gap material, the electronic structure of the SiNW becomes strongly dependent on its crystal orientation.[13] The transport features are thus expected to also manifest an orientational dependence, and although the diameters of the nanowires chosen in this study remain small (Fig. 1), most of the obtained results should remain be robust upon diameter and temperature upscaling within the limit of a few sub band and a diameter of $d <$?? nm. The van Hove singularities (VHs) seen in the SiNW DoS, related to subband extrema, degrades upon the introduction of SRD and are replaced by diffuse peaks or even disappear altogether. This degradation of the VHs is related to the creation of localized states in the nanowire, with a high concentration around the former VHs. Thus we can expect poor transport properties in the vicinity of any subband onsets. For the conduction band, the bulk silicon have six band minima, located around $\pm 0.8\Gamma X$, which will fold differently depending on the nanowire crystal orientation. Each bulk minimum has a heavy longitudinal effective mass ($0.92m_0$) and a light transverse effective mass ($0.19m_0$) along and perpendicular to the X-direction, respectively. Both the [100] and [110] SiNWs have the conduction band minima at the Γ point with a second minimum at higher energies and away from the Γ point. The two minima can be inferred from the folding of the bulk bands and the orientation of the bulk effective mass in relation to the SiNW. These two minima will converge in energy as the diameter of the nanowire increases. On the other hand for the [111] SiNW the band minima is located at $k = \pm 0.4\pi/l$ for $R > 1.0$nm. Also worth noticing is that the lowest effective mass is found in the [110] SiNW for the conduction band and in the [111] SiNW for the valence band.

The Kubo-Greenwood method is employed to extract the intrinsic transport length scales (elastic scattering time $\tau_e(E)$, mean free path $\ell_e(E)$ and charge mobility $\mu(E)$) from the saturation of the quantum diffusivity.[19] The real-space methodology originally proposed in Ref. [19] has been adapted to a multi-orbital per site problem.[18] The mean free path (l_e) is a fundamental quantity which gives a measure of a materials structural quality. In Fig. 2 the mean free paths for electrons and holes are plotted as functions of energy. The

TABLE I: Basic band structure parameters for SiNWs oriented along [100], [110] and [111] directions: the wave vector (k), the band degeneracy (deg) and the effective mass (m^*). ($^\alpha$ Only minimum for $R < 1.0$ nm.)

		vb	cb	
	k	0	0	$\pm 0.4\pi/l$
[100]	deg	2	1	2
	m^*	$1.5m_0$	$0.2m_0$	$0.9m_0$
	k	0	0	$\pm 0.8\pi/l$
[110]	deg	1	1	1
	m^*	$0.2m_0$	$0.2m_0$	$0.9m_0$
	k	0	$^{(\alpha)}0$	$\pm 0.4\pi/l$
[111]	deg	1	$^{(\alpha)}1$	2
	m^*	$0.15m_0$	$^{(\alpha)}0.6m_0$	$0.4 - 0.6m_0$

energy-dependence of the MFP can be straightforwardly related to the band structure. Close to each band edge the degradation of the VHs will enhance the backscattering, which results in shorter MFPs. Indeed, for the conduction band, the maximum MFP is found between the first and second group of VHs for all three nanowire orientations. Both the [110] and [111] oriented SiNWs have a clear peak close to the bandgap while the peak for the [100] oriented SiNW is less pronounced and has a shorter maximum value. Increasing interband scattering will suppress the MFP for all nanowire orientations, at higher energies. For the valence band, only the [111] oriented nanowire shows a strong peak close to the band edge. The [110] oriented nanowire also present a peak close to the band edge, which is weak and is followed by an equally high second broader feature at lower energies. For the [100] oriented nanowire no single peak is found, instead there is a broad collection of peaks centered away from the band edge.

In the framework of the Landauer-Büttiker method [20, 21], the SiNW has a finite length and is coupled to ideal semi-infinite SiNW-based leads with a fixed radius taken as $R = R_0 + 0.2$ nm. The measured conductance $G(E)$ is proportional to the total transmission probability, computed from the SiNW Green function[20], which is recursively evaluated by a standard decimation technique.[22] To evaluate the effect of SRD in finite length SiNWs the conductance along the three nanowire orientations are computed and averaged over ten roughness profile configurations, using the Landauer-Büttiker approach. The averaged conductance for SiNWs with lengths of $L \approx 20$ nm and $L \approx 80$ nm are shown in Fig. 3. The strong backscattering effects at the onset of each new subband is particularly obvious for the first subband. It can be seen as a strong reduction of the conductance, around the band edge, as the length of the SiNW is increased. At energies away from the band edges the conductance appears less sensitive to surface roughness. A correlation between the MFP and conductance can easily be drawn. At energies with long MFP, the conductance

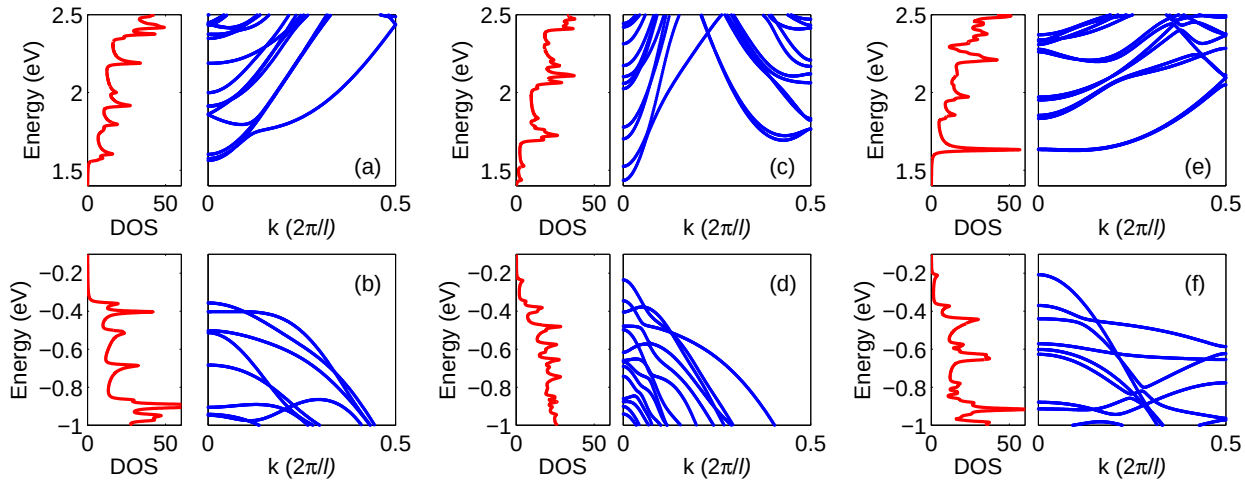

FIG. 1: Band structure and DOS for both the conduction and valence band calculated for ideal SiNWs oriented along the [100] [(a) and (b)], [110] [(c) and (d)] and [111] [(e) and (f)] crystal directions. All nanowires have a circular cross section with a diameter of 2 nm.

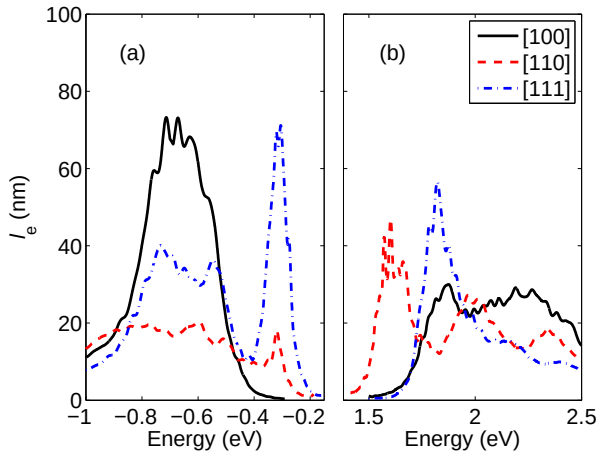

FIG. 2: Mean free path for electrons and holes in a $R_0 = 1$ nm SiNW with surface roughness. The mean free path is given for three nanowire orientations, [100] (black solid line), [110] (red dashed line) and [111] (blue dashed doted line).

still retains some hint of the conductance quantization (plateaus) of the ideal nanowire (shown as thin solid line in Fig. 3). The conduction bands of the [111] and [100] oriented nanowires are found to be highly sensitive to SRD in contrast to the [110] oriented SiNW. For the valence band the [100] oriented SiNW is the most sensitive to SRD, while both the [110] and [111] oriented SiNWs still retains a hint of the first conductance plateau.

Another important quantity for ascertaining the device performance is the charge carrier mobility ($\mu(E)$). Achieving high mobility is of great importance for engineering performant SiNW transistors, since it determines the switching speed of the device. It can be straightforwardly derived from the Kubo conductivity

$$\mu(E) = \frac{\sigma(E)}{n(E)e}, \tag{2}$$

where $n(E)$ is the charge density (per unit of length) and e is the elementary charge [19, 20]. Fig. 4 shows the room temperature mobility for the three nanowire orientations. Since the room temperature mobility becomes almost constant for Fermi energies inside the band gap, (low density mobility), it is a good quantity for evaluating transport efficiency. For the conduction band, the [110] oriented SiNW has the highest bandgap mobility, $\mu_{ld}^{cb} \approx 315\ cm^2V^{-1}s^{-1}$, which is in the same order as the experimental values for performant undoped SiNWs.[4]. As the Fermi energy is increased into the conduction band the mobility increases sharply towards a peak value of three times the low density mobility, $\mu_{max}^{cb} \approx 1040\ cm^2V^{-1}s^{-1}$. Both the [100] and [111] oriented nanowires have relatively low conduction band mobilities. For the valence band the [111] oriented SiNW has the highest mobility with a low density mobility of $\mu_{ld}^{vb} \approx 480\ cm^2V^{-1}s^{-1}$, followed by a sharp increase inside the valence band towards a peak mobility of $\mu_{max}^{vb} \approx 1340\ cm^2V^{-1}s^{-1}$. Thus the valence band of the [111] oriented nanowire has the highest mobility out of the three SiNW orientations. Also the [110] oriented SiNW has a high value for the low density mobility, but the value is in this case only about half of the [111] value and is not followed by a high peak mobility. The [100] oriented SiNW has a broad mobility peak located away from the band gap and a low value for the low density mobility. For both valence and conduction

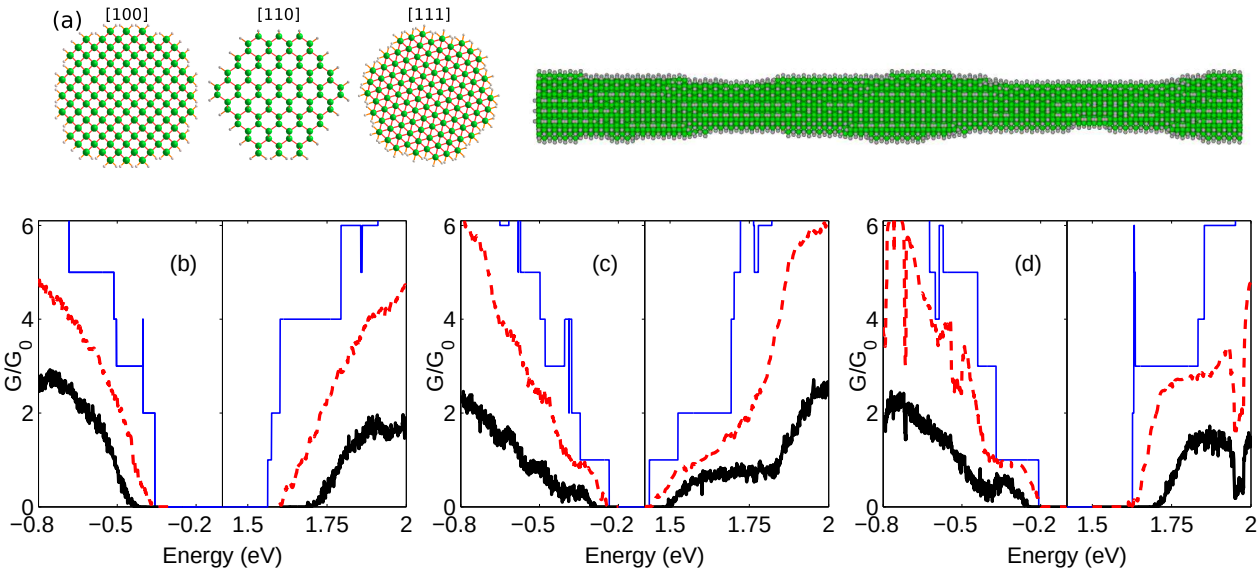

FIG. 3: (a) Cross-section for [100], [110] and [111] oriented nanowires and a typical example of surface roughness profile. (b-d) Conductance through SiNWs with SRD, for orientional growth along the [100] (b), [110] (c) and [111] (d) directions. Energy-dependent conductance for nanowire length $L \approx 20$ nm (red dashed line) and $L \approx 80$ nm (black solid line), the conductance has been averaged over ten SRD configurations. The quantized conductance for ideal (disorder-free) SiNWs(thin blue line) is shown shown.

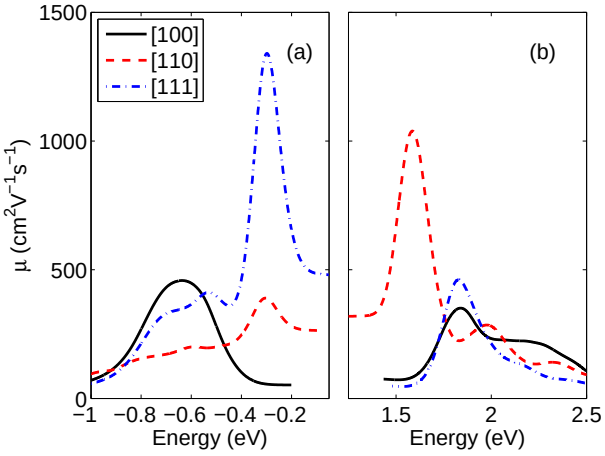

FIG. 4: Mobility for electrons and holes in a $R_0 = 1$ nm SiNW with SRD. The mobility is given at 300K for three crystal orientations, [100] (black solid line), [110] (red dashed line) and [111] (blue dashed doted line).

band the mobility at energies far away from the band gap tend to decrease owing to an increase in charge density and interband scattering.

The effect of SRD should be strongly dependent on the nanowire lateral size (radius), exhibiting little or negligible effect for large radius while showing strong enhancement of backscattering in smaller systems. To evaluate size effects, the mobility have been computed in the vicinity of the band gap for three different radius $R_0 = 0.5$, 1.0 and 1.5 nm for SiNWs oriented along the [110] direction. The low density mobility and the first mobility maximum, close to the band gap, are given in Table II. For small SiNWs, $R_0 \lesssim 1.0$ nm, the mobility is of the same order or smaller than the most performant SiNWs,[4] suggesting that SRD is the dominant scattering process in this size range. However, as the radius is increased the effect of SRD rapidly becomes less important. At $R_0 = 1.5$ nm the mobility is already larger than for the most performant undoped SiNWs, suggesting that other scattering mechanisms, e.g. chemical impurities and electron-phonon coupling, might be predominant for $R_0 \gtrsim 1.0$.

TABLE II: Maximum mobility and low density mobility, at 300K, close to the conduction and valence band for three SiNW radius, $R_0 = 0.5$, 1 and 1.5 nm, all oriented along the [110] direction. The the mobility is given in $cm^2V^{-1}s^{-1}$.

R_0	μ_{ld}^{cb}	μ_{ld}^{vb}	μ_{max}^{cb}	μ_{max}^{vb}
0.5	102	78	139	80
1.0	315	264	1040	390
1.5	1760	2275	2340	2400

The reported roughness-induced transport features will likely also extend to other types of surface disorders (trapped surface charges, or defects) since the energy-dependent backscattering profile can be traced to the electronic structure and not to the precise disorder modelling.

In conclusion, the effect of surface roughness on fundamental charge transport quantities have been studied for SiNWs oriented along the [100], [110] and [111] crystal directions. The study was carried out using a Landauer-Büttiker method in concert with a real space Kubo-Greenwood approach. The backscattering strength due to the surface roughness has been shown to be strongly influenced by the SiNW crystal orientation. The electronic structure for bulk silicon and SiNWs can be used to infer the major trends for conductance, mean free path and mobility. Electron transport along the [110] oriented nanowires was found to be least sensitive to roughness disorder while best hole transport efficiency was achieved for the [111] growth symmetry. Surface roughness disorder particularly enhances backscattering in small NW diameters. Finally, since the effect of surface disorder is strongly connected to the SiNWs electronic structure, our results should be applicable to other types of surface disorders.

This work was supported by the EU project No 015783 NODE, and the CEA ChimTronique programme. The calculations were performed at the CCRT supercomputing center.

[1] Xia Y.; Yang P.; Sun Y.; Wu Y.; Mayers B.; Gates B.; Yin Y.; Kim F.; Yan H. Adv. Mater. **2003**, *15*, 353.
[2] Cui Y.; Lieber C. M. Science **2001**, *291*, 851.
[3] Huang Y.; Duan X.; Cui Y.; Lauhon L. J.; Kim K.-H.; Lieber C. M. Science **2001**, *294*, 1313.
[4] Cui Y.; Zhong Z.; Wang D.; Wang W. U.; Lieber C. M. Nano Lett. **2003**, *3*, 149.
[5] Cui Y.; Wei Q.; Park H.; Lieber C. M. Science **2001**, *293*, 1289.
[6] Bertrand G.; Deleonibus S.; Previtali B.; Guegan G.; Jehl X.; Sanquer M.; Balestra F. Solid State Electronics **2004**, *48*, 505. Hofheinz M.; Jehl X.; Sanquer M.; Molas G.; Vinet M.; and Deleonibus S. Appl. Phys. Lett. **2006**, *89*, 143504.
[7] Colinge J. P. Sol. Stat. Elec. **2004**, *48*, 897.
[8] Goldberger J.; Hochbaum A. I.; Fang R.; Yang P. Nano Lett. **2006**, *6*, 973.
[9] Schmidt V.; Riel H.; Senz S.; Karg S.; Riess W.; Gösele U. Small **2006**, *2*, 85.
[10] Ma D. D. D.; Lee C. S.; Au F. C. K.; Tong S. Y.; Lee S. T. Science **2003**, *299*, 1874. Wu Y.; Cui Y.; Huynh L.; Barrelet C. J.; Bell D. C.; Lieber C. M. Nano Lett. **2004**, *4*, 433.
[11] van Langevelde R.; Klaassen F. M. IEEE Trans. Electron Devices **1997**, *44*, 2044. Sharma A. K.; Zaidi S. H.; Lucero S.; Brueck S. R. J.; Islam N. E. IEEE Proc.-Circuits Devices Syst. **2004**, *151*, 422.
[12] Wang J.; Polizzi E.; Ghosh A.; Datta S.; Lundstrom M. Appl. Phys. Lett. **2005**, *87*, 043101.
[13] Niquet Y. M.; Delerue C.; Allan G.; Lannoo M. Phys. Rev. B **2000**, *62*, 5109. Niquet Y. M.; Lherbier A.; Quang N. H.; Fernández-Serra M. V.; Blase X.; Delerue C. Phys. Rev. B **2006**, *73*, 165319.
[14] Rurali R.; Lorente N. Phys. Rev. Lett. **2005**, *94*, 026805.
[15] Fernandez-Serra M. V.; Adessi Ch.; Blase X. Phys. Rev. Lett. **2006**, *96*, 166805. *ibidem* Nano Lett. **2006**, *6*, 2674.
[16] Markussen T.; Rurali R.; Brandbyge M.; Jauho A-P. Phys. Rev. B. **2006**, *74*, 245313.
[17] Csontos, D.; Xu H. Q. Appl. Phys. Lett. **2000**, *77*, 2354. Zhong J.; Stocks G. M. Nano. Lett. **2006**, *6*, 128. Svizhenko A.; Leu P.W.; Cho K. Phys. Rev. B **2007**, *75*, 125417.
[18] Lherbier A.; Persson M.P; Niquet Y. M.; Triozon F.; Roche S. Phys. Rev. B **2008**, *77*, 085301.
[19] Roche S. Phys. Rev. B **1999**, *59*, 2284. Roche S.; Saito R. Phys. Rev. Lett. **2001**, *87*, 246803. Avriller R.; Latil S.; Triozon F.; Blase X.; and Roche S. Phys. Rev. B (RC) **2006**, *74*, 121406.
[20] Ferry D. K.; Goodnick S. M. *Transport in Nanostructures*, Cambridge University Press (Cambridge, U.K., 1997).
[21] Landauer R. IBM J. Res. Dev. **1957**, *1*, 223. Landauer R. Philos. Mag. **1970**, *21*, 863. Bütiker; and Landauer R. Phys. Rev. Lett. **1982**, *49*, 1739.
[22] Grosso G.; Moroni S.; Parravicini G. P. Phys. Rev. B **1989**, *40*, 12328. Triozon F.; Lambin Ph.; Roche S. Nanotechnology **2005**, *16*, 230.
[23] Allan G. J. of Phys. C: Solid State Phys. **1984**, *17*, 3945.
[24] Weiße A.; Wellein G.; Alvermann A.; Fehske H. Rev. Mod. Phys. **2006**, *78*, 275.
[25] Thouless D. J. Phys. Rev. Lett. **1977**, *39*, 1167.
[26] Beenakker C. W. J. Rev. Mod. Phys. **1997**, *69*, 731.
[27] Dong J.; Drabold D. A. Phys. Rev. Lett. **1998**, *80*, 1928.